Insights into the mechanism of methylene blue removed by novel and classic biochars

Wei Chen, Fengting Chen, Bin Ji, Lin Zhu and Hongjiao Song

ABSTRACT

The adsorption behavior and the underlying mechanism of methylene blue (MB) sorption on biochars prepared from different feedstocks at 500 °C were evaluated. The biochar feedstocks included *Magnolia grandiflora* Linn. leaves biochar (MBC), pomelo (*Citrus grandis*) peel biochar (PBC) and badam shell biochar (BBC). The results of characterizing and analyzing the samples showed that different biochars had different effects on the adsorption of MB. It could be found that MBC had the best adsorption effect on MB due to its largest average pore diameter of 5.55 nm determined by Brunauer-Emmett-Teller analysis. Under the optimal conditions, the maximum adsorption capacities of BBC, PBC and MBC were 29.7, 85.15 and 99.3 mg/g, respectively. The results showed that the amount of adsorption was affected by the pH value. The maximum adsorption capacity of MBC was 46.99 mg/g when it was at pH of 3, whereas for the same experimental conditions the maximum adsorption capacity of BBC and PBC was 25.29 mg/g at pH of 11 and 36.08 mg/g at pH of 7, respectively. Therefore, MBC was found to be a most efficient low-cost adsorbentl for dye wastewater treatment compared with BBC and PBC, and it had the best removal effect under acidic conditions.

Key words | adsorption, biochar, isotherm, kinetic, methylene blue

Wei Chen
Fengting Chen
Bin Ji
Lin Zhu
Hongjiao Song (corresponding author)
School of Urban Construction,
Wuhan University of Science and Technology,
Wuhan 430081,
China
E-mail: *songhongjiao@wust.edu.cn*

Bin Ji
Hubei Key Laboratory for Efficient Utilization and Agglomeration of Metallurgic Mineral Resources,
Wuhan University of Science and Technology,
Wuhan, 430081,
China

INTRODUCTION

Many industrial processes involving a large amount of dyes cause the formation of dye wastewater, such as textiles, leather nitrification, paper production and food technology (Tan *et al.* 2007). With the rapid development of the chemical industry in our country, large amounts of dye wastewater have been directly discharged into the environment which has caused negative consequences to the environment and human health. Methylene blue (MB) is a common basic dye which has very large applications for dyeing cotton, wool and clothing besides having a great use in medicine and colored paper. Acute intake of a large amount of MB would cause heart rate increase, vomiting, shock, purpura, jaundice, limb paralysis and tissue gangrene (Lyu *et al.* 2018). In addition, high dose MB could induce methemoglobinemia, lead to Heinz-body anemia or other symptoms of red cell morphology change and reduce red blood cell life. Therefore, it is an urgent and important global problem to effectively remove dyes.

Dye wastewater treatment methods mainly include coagulation and flocculation, chemical oxidation, membrane separation and adsorption (Rafatullah *et al.* 2010). Among them, adsorption technology is widely used in the treatment of dye wastewater because of its easy handling, low cost and high efficiency. Adsorption is considered as a valid method for balanced separation and water purification applications (Harikishore Kumar Reddy *et al.* 2017). Activated carbon can effectively remove active, alkaline and azo dyes in wastewater. However, it is generally applied to dye wastewater treatment or advanced treatment with lower concentration due to its difficulty in regeneration and high cost. In recent years, domestic and foreign scholars have begun to look for new cheap adsorbent materials to try to replace activated carbon. Biomaterials had been found to have the advantages of low price, easy availability, wide application conditions and abundant sources. Waste plant materials also have adsorption potential and can be used as biosorbents. The cell wall of plant materials is rich in lignin, cellulose and hemicellulose. The main reason for the adsorption of dyes by plant materials is that their cellulose and hemicellulose are rich in hydroxyl groups and polyphenol groups. These groups can adsorb dye molecules

doi: 10.2166/wst.2019.158

through different mechanisms such as electrostatic adsorption, complexation and hydrogen bonding.

This paper describes the use of pomelo (*Citrus grandis*) peel (fruit peel), badan shell (dried fruit shell) and *Magnolia grandiflora* Linn. leaves (woody plant) as raw materials to study the adsorption behavior of MB. Firstly, the factors affecting the adsorption effect were investigated, and then the adsorption process was optimized by analyzing various parameters of adsorption kinetics. The purpose of this study was to explore the adsorption efficiency and adsorption process of three biochars, and to measure and compare the differences in adsorption capacity of dyes on biochars.

MATERIAL AND METHODS

Preparation of biochars

Magnolia grandiflora Linn. leaves were taken from a local tree (30° 26′ 48″ N, 114° 15′ 25″ E), pomelo (*Citrus grandis*) peel was obtained from a local fruit market (30° 34′ 56″ N, 114° 25′ 38″ E) and badam shell was purchased from Urumqi (43° 50′ 10″ N, 7° 37′ 24″ E), Xinjiang, China. The raw materials were naturally dried first, soaked in deionized water to remove surface impurities, and placed in an oven to dry at 80 °C. Then these biochars were pyrolyzed in a tubular furnace under anoxic conditions at 500 °C. After the pyrolysis residue was cooled to room temperature, it was ground into powder to pass through a 100-mesh sieve and then rinsed repeatedly with distilled water to neutral. It was put in the oven and dried to constant weight at 80 °C. Finally, it was stored in plastic bottles for later use. The biochars prepared from three different raw materials are named *Magnolia grandiflora* leaves biochar (MBC), pomelo peel biochar (PBC) and badam shell biochar (BBC), respectively.

Chemicals

MB supplied by Sinopharm Chemical Reagent Co., Ltd was used as an adsorbate without further purification. A certain amount of MB solid was obtained, and then formulated into a 300 mg/L solution with distilled water as stock solution. Solutions of the corresponding mass concentration were diluted proportionally with deionized water accordingly.

Batch sorption experiment

Batch adsorption studies were conducted by adding equal amounts of biochars (0.10 g) to a series of identical 100 mL plastic bottles containing 100 mL MB solution (20–200 mg/L) under an oscillating incubator (ZQTY-70S, Shanghai, China), at a certain temperature (293, 298, 303 K) to achieve equilibrium of the solution for 24 h. Then the solutions were shaken at 150 rpm. A sample was extracted from the solution at appropriate intervals. The solution obtained by filtering through a 0.22 μm filter (polyethersulfone membrane) was used to determine the concentration of MB, which was measured by using a UV-vis spectrophotometer (A 580, Shanghai, China) at maximum wavelengths of MB (665 nm). The equilibrium adsorption capacity (q_e) of dyes and the removal efficiency of MB on biochars were obtained by the following equations, respectively.

$$q_e = \frac{(C_0 - C_e)V}{W} \times 100 \quad (1)$$

$$\text{Removal percentage} = \frac{(C_0 - C_e)}{C_0} \times 100 \quad (2)$$

where C_0 and C_e (mg/L) are the concentrations of MB in the liquid phase at initial and equilibrium, respectively. V (L) is the volume of the solution and W (g) is the mass of adsorbent used.

Effect of solution pH

The effect of pH on adsorption was studied by adsorption studies under different pH conditions. The initial concentration of 100 mL dye solution was set to 50 mg/L, adjusted to different pH values (pH 2, 3, 5, 7, 9, and 11), and 0.1 g of biochar was added. The pH was measured by using a pH meter (ST3100, Changzhou, China). Then, the solution was placed in a constant temperature oscillator and controlled. After shaking for 24 h, the sample was taken out and the amount of adsorption at this time was measured.

Kinetics studies

For the kinetic experiment, 1.0 g of sorbent was mixed with 100 mL of MB solution (C_0: 70 mg/L, 150 mg/L) at pH 5. While the temperature was maintained at 298 K, the agitation speed was set at 150 rpm and 2.0 mL solution was extracted with a disposable needle filter (0.45 μm) at

regular intervals. Then the residual concentrations were determined and the samples were analyzed.

Different kinetic models were used to study the rate control mechanism of MB adsorption onto three biochars. The experimental data were fitted using OriginPro 8.5.1 software to establish a kinetic model. The merits of the model are evaluated by the coefficient of determination R^2 and chi square χ^2. The closer R^2 is to 1 and the smaller the χ^2, the better the equation matching.

$$\chi^2 = \frac{1}{n}\sum \frac{(Q_{exp} - Q_{cal})^2}{Q_{cal}} \quad (3)$$

where n is the number of data points, while Q_{exp} and Q_{cal} represent the experimental and the calculated values of equilibrium sorption capacity respectively.

All experiments were repeated three times, and the experimental error limit of three experiments is ±5%.

RESULTS AND DISCUSSION

Physical–chemical properties of biochar

Biochar particles were characterized by scanning electron microscopy, Fourier transform infrared spectroscopy and Brunauer–Emmett–Teller (BET) analysis. The BET specific surface area of PBC was very small at 0.026 m^2/g and BJH (Barrett-Joyner-Halenda) desorption cumulative volume of pores was 0.00145 cm^3/g. The BET surface area, total pore volume and average pore diameter of the BBC were found to be 269.02 m^2/g, 0.13532 cm^3/g and 3.2554 nm, respectively, and for MBC were 98.89 m^2/g, 0.028 cm^3/g and 5.55 nm, respectively. It can be seen that the average pore diameter of the MBC is the largest. Table 1 lists these results.

The Fourier transform infrared (FTIR) spectra of different biochars are listed in Figure 1. The FTIR spectra obtained showed that the functional groups of biochar samples after adsorption had changed, and some peaks

Table 1 | BET analysis data

Adsorbent type	BET surface area m^2/g	Total pore volume cm^3/g	Adsorption average pore diameter nm
PBC500	0.026	0.00145	–
BBC500	269.02	0.1353	3.2554
MBC500	98.89	0.028	5.55

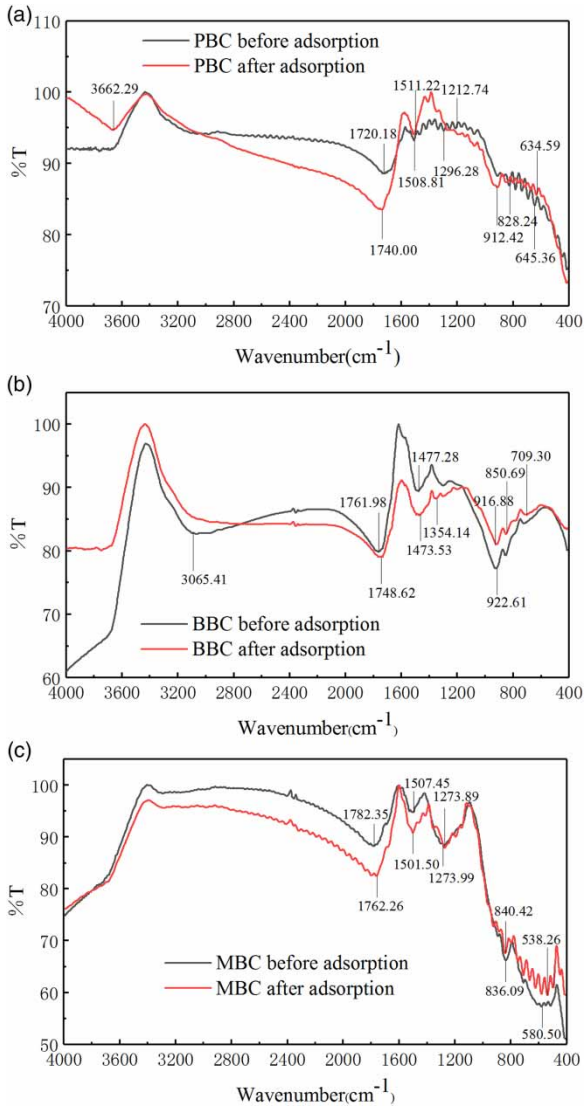

Figure 1 | FTIR spectra of different biochars: (a) pomelo (*Citrus grandis*) peel biochar, (b) badam shell biochar, (c) *Magnolia grandiflora* Linn. leaves biochar.

disappeared while new peaks appeared. For BBC, the medium peak near 3,065.41 cm^{-1} indicated the presence of –OH stretching. Various bands in the spectrum were identified as corresponding to the C=O stretching (at wavenumber of 1,761.98 cm^{-1}), the C–H bending (1,477.28 cm^{-1}) and the symmetric bending of C–O–C (922.61 cm^{-1}). Figure 1(a) shows the FTIR spectra of PBC. The FTIR analysis indicated that there was a distinct absorption peak at 3,662.29 cm^{-1}, representing the stretching vibration absorption of –OH groups. It indicated that a large amount of hydroxyl groups existed in the pomelo peel. A strong peak at 1,740 cm^{-1} was due to C=O stretching, which indicated that the pomelo peel contains carbonyl. These carbonyls are likely to come from acids or esters since

the pomelo peel contains a lot of cellulose and pectin. A peak at 1,511.22 cm^{-1} was considered to be due to the presence of alkene (C–H) bending. A peak at 912.42 cm^{-1} could be due to symmetric bending of C–O–C and a medium peak at 643.59 cm^{-1} signified C–OH twist. For MBC, the band at 1,782.35 cm^{-1} could be due to C=O stretching and the medium band at 1,507.45 cm^{-1} to C–H bending. The peak around 1,273.69 cm^{-1} corresponded to the C–O–C stretching. Moreover, the medium peak at 836.09 cm^{-1} was caused by C–H bending (out of the plane). The peak at 580.5 cm^{-1} was the C–C group. The strengths of C–H and C=O decreased significantly before and after adsorption, indicating that these groups are the main reactive groups of these three biochars interacting with MB.

To further explore the surface structure of the samples, the BC samples before and after adsorption were observed with scanning electronic microscopy (SEM) and energy dispersive spectroscopy (EDS). The results are shown in Figure 2. It could be seen from Figure 2(a), 2(c) and 2(e) that the prepared adsorbent has a rich pore network structure, and the pore distribution is uniform and dense, which ensured that the sample has a high specific surface area and pore volume (Esquena 2012). The surface of dye-loaded adsorbent (Figure 2(b), 2(d) and 2(f)), indicates that the surface of biochars was covered with material. The structure of PBC was similar to that of MBC because of their fibre structure. The pore in BBC was smaller than that in PBC and MBC. Their elemental compositions were further investigated by EDS spectrum. The elements of different biochars are basically unchanged after adsorption, indicating that these elements do not participate in reactions. The types of elements of different biochars are also inconsistent.

Effects of contact time and initial dye concentration

The effects of contact time and initial dye concentration on the adsorption of MB by biochar were studied. It could be seen from Figure 3 that the adsorption amount of MB on three biochars increased with time. The adsorption results of the three biochars showed that the amount of biochars adsorbed to MB increased rapidly with time at the beginning of the reaction, and then the amount of adsorption changed slowly and gradually stabilized. It was because there were a large number of empty positions on the surface of the biochar for adsorption in the initial stage, and when the reaction was in process, the remaining empty surface positions become more and more difficult to occupy due to the repulsive force between the solute molecules (Jia *et al.* 2018). When the initial concentrations of MB were 70 mg/L and 150 mg/L, the adsorption amount of MB on adsorbent increased rapidly in the first 60 min. The results showed that the rate of dye adsorption was fast. It could be due to the electrostatic attraction between biochar and MB. When the initial MB concentration was changed from 20 to 200 mg/L under certain external adsorption conditions, the removal rate of MB decreased as the initial concentration of the solution increased. This phenomenon was related to the mass transfer driving force (Sadaf & Bhatti 2014). The adsorption load increases as the concentration of the MB solution increases, which was not conducive to promoting the diffusion of the adsorbate from the liquid to the surface and inside of the adsorbent, causing a decrease in adsorption rate (Dhodapkar *et al.* 2007). The results showed the removal efficiency of BBC had the largest change, which decreased from 92.06% to 9.63%.

Adsorption kinetics

MB adsorption characteristics were compared based on adsorption studies on biochar particles at different times. For biochar samples, MBC showed the best adsorption performance. In order to better understand the kinetics of MB adsorption on the three biochars, the pseudo-first-order kinetic equation and pseudo-second-order kinetic equation were used to fit the adsorption process, and then the appropriate kinetic model of the adsorption process could be determined. The pseudo-first-order and pseudo-second-order models were used to represent single-nuclear and dual-nuclear adsorption processes in solid solution systems, respectively (Chen *et al.* 2018). The pseudo-first-order equation (Mosa *et al.* 2018) is expressed in the form:

$$\ln(q_e - q_t) = \ln q_e - k_1 t \tag{4}$$

where q_e is the equilibrium adsorption capacity (mg/g), k_1 is the pseudo-first-order kinetic rate constant, t is the adsorption time (min) and q_t is the adsorption capacity at t time (mg/g). The pseudo-first-order kinetic equation was obtained by drawing the linear plots of $\ln(q_e - q_t)$ versus t (Figure 4(a)).

The corresponding parameters are listed in Table 2. The correlation coefficient values of pseudo-first-order were relatively small. This indicated that the adsorption of MB on the biochars does not belong to the pseudo-first-order equation (Elmorsi *et al.* 2017). The pseudo-second-order dynamic

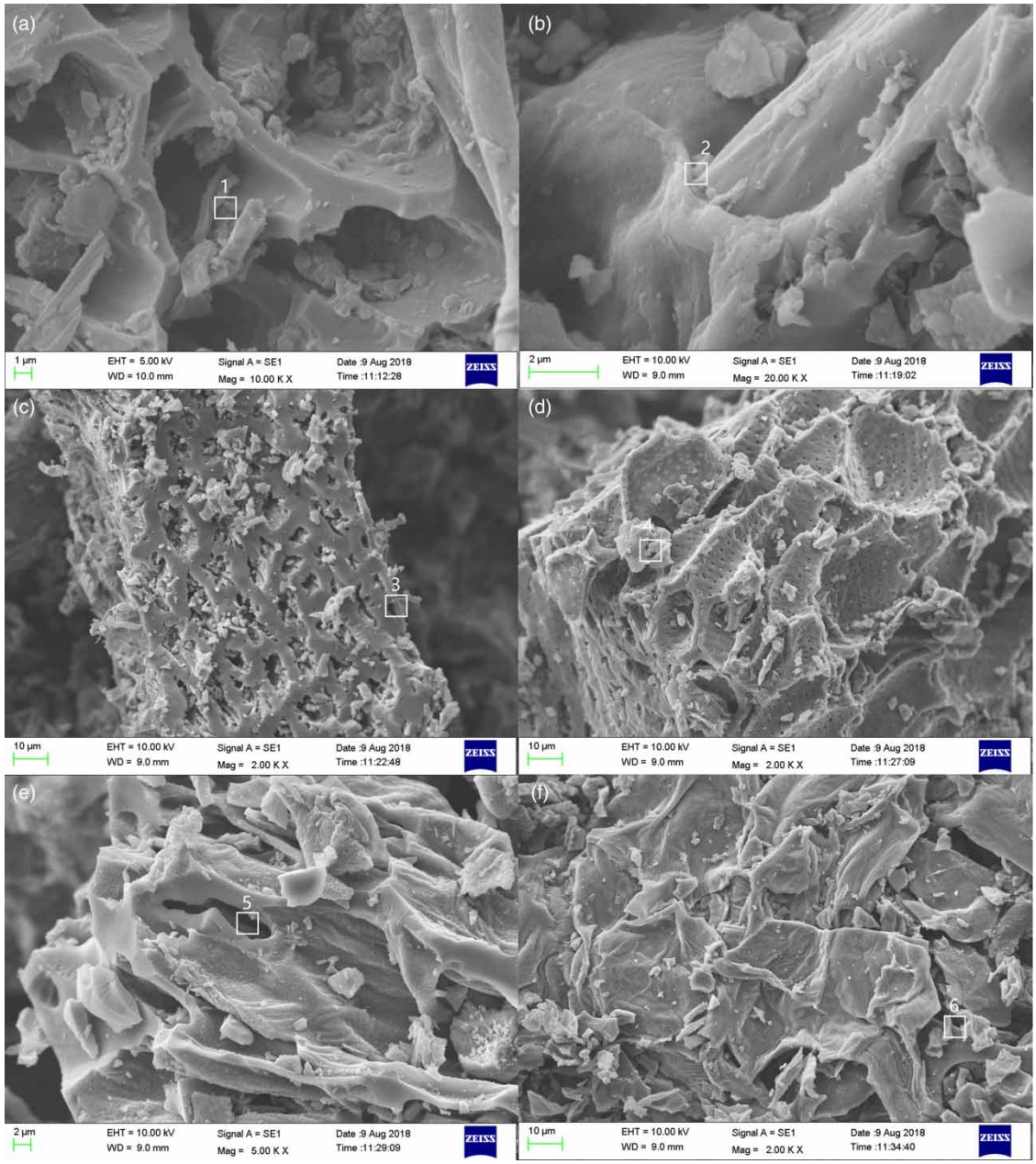

Figure 2 | (a) SEM of *Magnolia grandiflora* Linn. leaves biochar before adsorption. (b) SEM of *Magnolia grandiflora* Linn. leaves biochar after MB adsorption. (c) SEM of pomelo (*Citrus grandis*) peel biochar before adsorption. (d) SEM of pomelo (*Citrus grandis*) peel biochar after MB adsorption. (e) SEM of badam shell biochar before adsorption. (f) SEM of badam shell biochar after MB adsorption.

equations can be expressed in the following form:

$$\frac{t}{q_t} = \frac{1}{k_2 q_e^2} + \left(\frac{1}{q_e}\right)t \tag{5}$$

where k_2 (g/(mg min)) is the rate constant of the pseudo-second-order reaction, and can be obtained through the slope and intercept of plot t/q_t against t (Figure 4(b)).

The correlation coefficient associated with the linear fit and the average chi-square error (χ^2) analysis were used to evaluate the best model describing the MB adsorption data (Elwakeel *et al.* 2017). χ^2 is determined according to Equation (3). The kinetic parameters are listed in Table 2. It could be seen from Figure 4(a) and 4(b) that the pseudo-first-order kinetic adsorption data slightly deviated from the fitting curve, and the correlation coefficient R^2 was

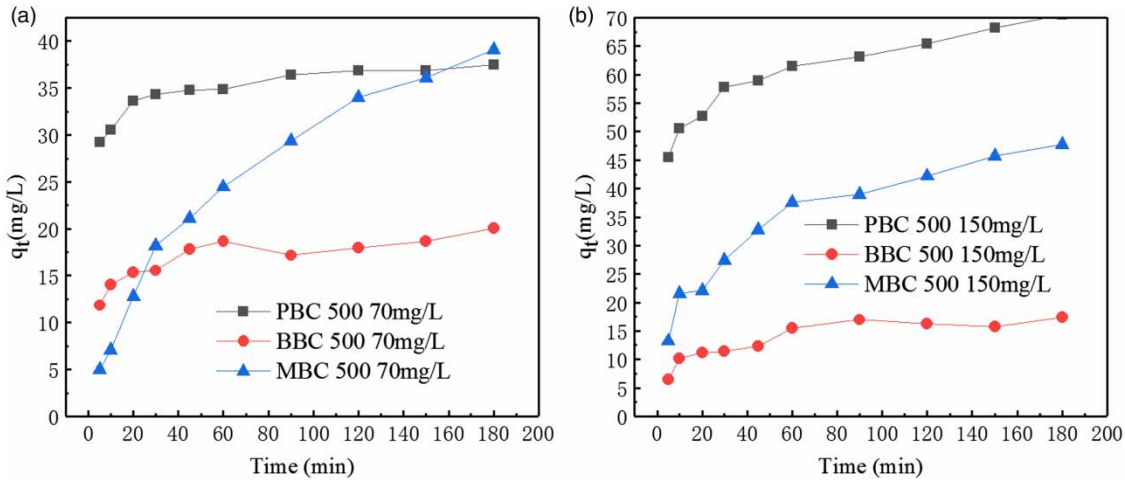

Figure 3 | The variation of adsorption capacity with adsorption time: (a) at 70 mg/L initial MB concentrations, (b) at 150 mg/L initial MB concentrations (t = 298 K, w = 0.10 g, v = 100 mg/L).

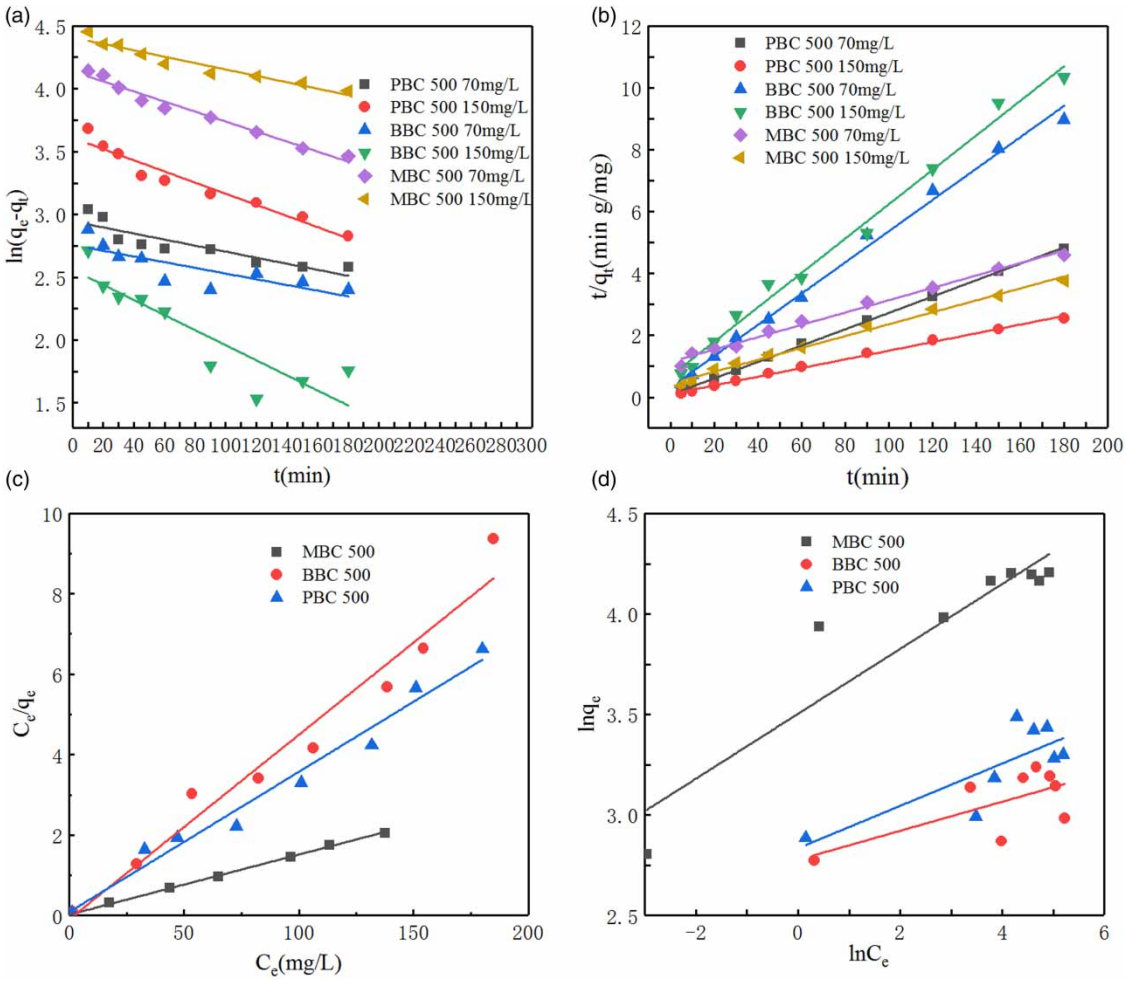

Figure 4 | (a) Pseudo-first-order kinetics for adsorption of various initial MB concentrations onto different biochars at 298 K. (b) Pseudo-second-order kinetics for adsorption of various initial MB concentrations onto different biochars at 298 K. (c) Langmuir isotherms for MB dye adsorption onto different biochars at 298 K. (d) Freundlich isotherms for MB dye adsorption onto different biochars at 298 K.

Table 2 | Kinetic parameters of the pseudo-first-order and pseudo-second-order equations for MB adsorption onto biochars from different feedstock

		Pseudo-first-order			Pseudo-second-order		
Sorbent	**C_0 (mg/L)**	**Q_e (mg/g)**	**k_1**	**R^2**	**Q_e (mg/g)**	**k_2**	**R^2**
PBC 500	70	19.51	0.0024	0.7766	37.74	0.0091	0.9997
PBC 500	150	38.10	0.0050	0.9469	70.92	0.0020	0.9971
BBC 500	70	16.33	0.0026	0.7250	17.99	0.0046	0.9912
BBC 500	150	12.50	0.0063	0.7859	19.76	0.0082	0.9942
MBC 500	70	65.36	0.0044	0.9624	50.00	0.0004	0.9907
MBC 500	150	87.33	0.0027	0.9066	52.08	0.0008	0.9906

0.7250–0.9624. The fitting effect of the pseudo-second-order kinetic equation was relatively good, and the adsorption data were basically consistent with the fitting curve. The calculation shows that the average chi-square error (χ^2) of the pseudo-second-order kinetic equation was smaller than that of the pseudo-first-order kinetic equation. R^2 was 0.9906–0.9997. This phenomenon indicated that the adsorption mechanism of biochar for the MB solution was diverse but it was still based on chemistry (Smith *et al.* 2016). The adsorption mechanism of biochar for organic pollutants mainly includes distribution and surface adsorption, and also includes other microscopic adsorption mechanisms. The pseudo-second-order kinetic model provides a better fit than the pseudo-first-order model, suggesting that MB adsorption to these biochars might involve a multi-nucleus rather than single-nucleus adsorption process. Similar phenomena were reported for malachite green adsorption onto sugarcane bagasse biochar (Vyavahare *et al.* 2018) and removal of levofloxacin using rice-husk and wood-chip biochars (Yi *et al.* 2016).

Adsorption equilibrium

The adsorption isotherm is an important basis for analyzing the adsorption process. It is used to describe the affinity and the adsorption capacity of the adsorbent (Latour 2015). The adsorption isotherm also has important value in estimating and interpreting thermodynamic parameters and judging the interaction between adsorbent and adsorbate. To further study the adsorption behavior of MB on the surface of these biochars, the Langmuir and Freundlich isotherm adsorption models were used to fit the MB adsorption isotherm data. The adsorption isotherm could reflect the distribution of liquid phase and the solid phase for adsorbed molecules when the adsorption process was in equilibrium (Hartig *et al.* 2017). The R^2 values were used to determine the degree of fitting of the isotherm equation to the adsorption of MB by these three biochars. The higher the R^2 values, the better the isotherm data fit. The Langmuir adsorption model assumes that a monolayer covers the surface of the adsorbent, and the adsorbate has the same force on the solid surface and has no interaction with each other. The linear equation of the Langmuir adsorption model is expressed as follows:

$$\frac{C_e}{q_e} = \frac{1}{Q_0 b} + \frac{C_e}{Q_0} \tag{6}$$

where C_e (mg/L) is the concentration of the adsorbate in the solution at the equilibrium of adsorption, q_e (mg/g) is the adsorption amount when the adsorption reaches equilibrium, Q_0 is the saturated adsorption amount (mg/g) and b is the Langmuir constant related to the affinity and adsorption energy of the bonding site (L/mg). The Freundlich isotherm model is based on multi-layer adsorption on heterogeneous surfaces (Bhaumik *et al.* 2014). The expression of the Freundlich isotherm equation (Chen *et al.* 2018) is shown below:

$$\ln q_e = \ln K_F + \frac{1}{n} \ln C_e \tag{7}$$

where K_F (mg/g) is a constant related to the adsorption capacity and the adsorption strength under the Freundlich model and $1/n$ (L/mg) is a measure of the adsorption intensity. The value of $1/n$ is generally between 0 and 1, and its value indicates the influence of the concentration on the amount of adsorption. The smaller the $1/n$ is, the better the adsorption performance (Ahmaruzzaman 2008). Larger K_F and n values are indicative of better adsorption properties of the adsorbent. Freundlich adsorption isotherms were obtained by plotting $\ln q_e$ against $\ln C_e$, respectively.

The R^2 values and the constants of two isotherm models for MB adsorption on BBC, PBC and MBC at

298 K are listed in Table 3. The results showed that the linear correlation coefficient of the Langmuir isotherm equation was 0.9626–0.9986, which was higher than the linear correlation coefficient fitted by the Freundlich isotherm equation. It could be seen from Figure 4(c) and 4(d) that the Langmuir model could better describe the MB adsorption behavior of these biochars. The Langmuir adsorption model proved that these three kinds of biochar as adsorbents had an abundant-pore structure and uniform adsorption point distribution, and mainly monolayer adsorption occurred between MB molecules and biochar.

Similar results were reported for MB adsorption on activated carbon made of dehydrated peanut hull (Özer *et al.* 2007). The result that the equilibrium parameter R_L values were between 0 and 1 showed that these biochars were beneficial for the adsorption of MB under the experimental condition. The maximum adsorption capacities of BBC, PBC and MBC were 25.52, 32.71 and 67.05 mg/g, respectively. The adsorption capacities of BBC and PBC were close, and the value of MBC was highest.

Effect of temperature on dye adsorption

The temperature has an effect on the adsorption amount of adsorbent. The diffusion rate of the adsorbed molecules through the outer boundary layer and the internal pores of the adsorbed particles increased with increasing temperature (Al-Qodah 2000). As the temperature increased, the adsorption behavior of BBC, PBC and MBC was also different. For BBC, the adsorption capacity decreased with increasing temperature. It indicates that the process of BBC adsorbing MB is exothermic. This was because the physical bond between the MB and the active site of the adsorbent decreased as the temperature increased. It showed that MB was adsorbed onto the BBC, which caused the adsorbate molecules to lose some degrees of freedom. Similar trends were reported for adsorption of MB on activated carbon prepared from coconut husk (Tan *et al.* 2008).

Completely different behaviors were obtained for PBC and MBC; the amount of adsorption became larger as the temperature increased, which meant that the adsorption of MB by both biochars was an endothermic process. This may be caused by the increase of the migration rate of dye molecules and the number of active centers as the temperature increased (Salleh *et al.* 2011). Thus more and more molecules got enough energy to interact with the active center on the surface.

Effect of solution pH on dye adsorption

The pH value of the solution is one of the important factors affecting the adsorption performance of the adsorbent since the pH in the solution not only affects the existent morphology of MB cations in solution but also affects the active sites on the surface of the adsorbent (Khattri & Singh 2009). The effect of pH on biochar adsorption was investigated at an initial dye concentration of 50 mg/L, an oscillation time of 24 h, and BC concentration and temperature fixed at 0.10 g and 298 K, respectively. The effect of pH on MB adsorption under equilibrium (q_e) is shown in Figure 5(a). For PBC and BBC, a low amount of dye was found to be adsorbed when the solution was in low pH. MB is a cationic dye: a large amount of H^+ in the solution will compete and occupy the adsorption site when in low pH, resulting in a low adsorption rate. At near-neutral pH conditions, the surface of the adsorbent would accumulate more negative charges to promote adsorption between the positive dye ions and the adsorbent through electrostatic interaction. As the pH rises, the adsorption effect increases slowly. At pH of 7 the adsorption capacity of PBC was at maximum (36.08 mg/g) whereas the maximum adsorption capacity of BBC was 25.29 mg/g at pH 11. Nevertheless, MBC at high pH value showed a slight decrease in dye adsorption. The maximum adsorption capacity of MBC was 46.99 mg/g at pH of 3. There might be other adsorption mechanisms such as ion exchange or chelation (Hamdaoui 2006). Similar results

Table 3 | Parameters of Langmuir equation and Freundlich equation

	Freundlich equation			Langmuir equation		
Sorbent	K_F	n	R^2	Q_0	b	R^2
PBC 500	17.89	8.9206	0.6570	28.65	0.4072	0.9750
BBC 500	17.11	13.8504	0.4614	21.79	−0.4826	0.9626
MBC 500	35.94	6.1996	0.8689	66.67	0.6849	0.9986

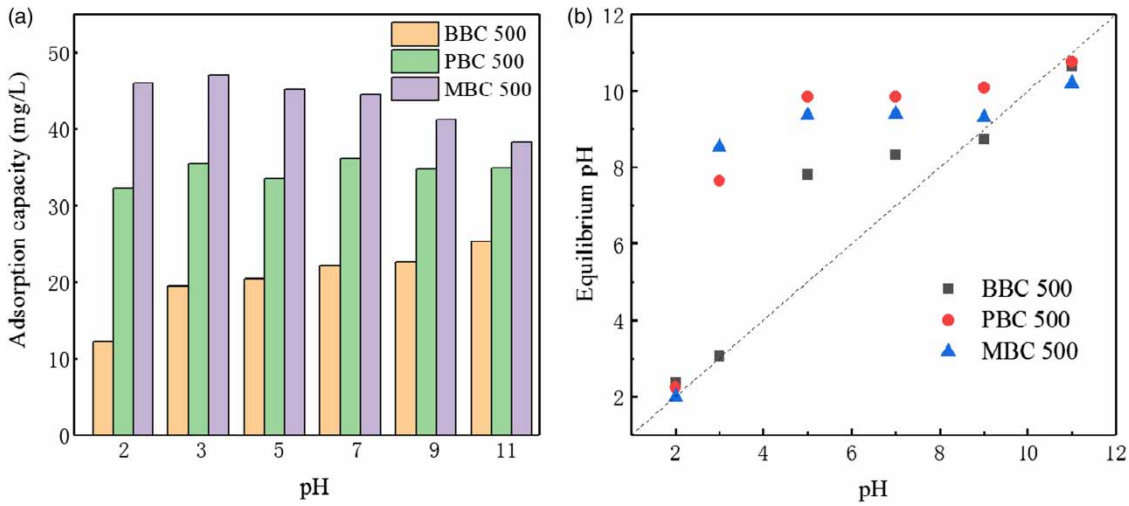

Figure 5 | (a) Effect of pH on MB sorption by biochars. (b) The pH change of the mixed solution of BCs with MB after equilibration ($T = 298$ K, $C_0 = 50$ mg/L, $W = 0.10$ g, $V = 100$ mg/L).

were observed for the adsorption of MB on cedar sawdust and broken bricks (Hamdaoui 2006). As shown in Figure 5(b), the pH of the equilibrium solution was increased compared to the initial pH because the addition of biochars, which usually had an alkaline pH, neutralized the acidity of the solution.

CONCLUSIONS

The research shows that the BBC, MBC and PBC all could be used to remove MB dye as a cheap and available adsorbent. The adsorption of MB onto MBC was found to be more effective than that of BBC and PBC. The amount of MB uptake on BBC, MBC and PBC increased with increasing of initial dye concentration and contact time. It was observed that the pH dependency of adsorption by BC was large. The above phenomena of the three adsorbents suggested adsorption of MB on MBC and PBC was endothermic while exothermic for BBC. The adsorption isotherms of BBC, PBC and MBC for MB were in accordance with the Langmuir equation and belong to monolayer adsorption. Their maximum adsorption capacities were 29.7, 85.15 and 99.3 mg/g, respectively. The adsorption kinetics were consistent with the pseudo-second-order kinetics models. The maximum adsorption capacities of PBC and MBC were close to each other and both higher than BBC. It was found that MBC has the best adsorption effect on MB, indicating that MBC could be used as the best biological material for dye wastewater treatment compared with BBC and PBC.

ACKNOWLEDGEMENTS

This research was financially supported by the Project (2017zy011) of Hubei Key Laboratory for Efficient Utilization and Agglomeration of Metallurgic Mineral Resources, the Natural Science Foundation of Hubei Province of China (2017CFB350). Also the authors would like to thank teacher Zhou for support with the BET and FTIR analysis.

REFERENCES

Ahmaruzzaman, M. 2008 Adsorption of phenolic compounds on low-cost adsorbents: a review. *Adv. Colloid Interface Sci.* **143**, 48–67.

Al-Qodah, Z. 2000 Adsorption of dyes using shale oil ash. *Water Res.* **34**, 4295–4303.

Bhaumik, M., Choi, H. J., Seopela, M. P., McCrindle, R. I. & Maity, A. 2014 Highly effective removal of toxic Cr(VI) from wastewater using sulfuric acid-modified avocado seed. *Ind. Eng. Chem. Res.* **53**, 1214–1224.

Chen, Y., Lin, Y., Ho, S., Zhou, Y. & Ren, N. 2018 Highly efficient adsorption of dyes by biochar derived from pigments-extracted macroalgae pyrolyzed at different temperature. *Bioresour. Technol.* **259**, 104–110.

Dhodapkar, R., Rao, N. N., Pande, S. P., Nandy, T. & Devotta, S. 2007 Adsorption of cationic dyes on jalshakti, super absorbent polymer and photocatalytic regeneration of the adsorbent. *React. Funct. Polym.* **67**, 540–548.

Elmorsi, T. M., Elsayed, M. H. & Bakr, M. F. 2017 Enhancing the removal of methylene blue by a modified ZnO nanoparticles, kinetics and equilibrium studies. *Can. J. Chem.* **95**, 1–11.

Elwakeel, K. Z., Elgarahy, A. M. & Mohammad, S. H. 2017 Use of beach bivalve shells located at Port Said coast (Egypt) as a green approach for methylene blue removal. *J. Environ. Chem. Eng.* **5**, 578–587.

Esquena, J. 2012 Drug delivery properties of macroporous polystyrene solid foams. *J. Pharm. & Pharm. Sci.* **15**, 197–207.

Hamdaoui, O. 2006 Batch study of liquid-phase adsorption of methylene blue using cedar sawdust and crushed brick. *J. Hazard Mater.* **135**, 264–273.

Harikishore Kumar Reddy, D., Vijayaraghavan, K., Kim, J. A. & Yun, Y. 2017 Valorisation of post-sorption materials: opportunities, strategies, and challenges. *Adv. Colloid Interface Sci.* **242**, 35–58.

Hartig, D., Schwindt, N. & Scholl, S. 2017 Using the local adsorption equilibrium distribution based on a Langmuir type adsorption model to investigate liquid phase adsorption of sugars on zeolite BEA. *Adsorption* **23**, 433–441.

Jia, Y., Shi, S., Jie, L., Su, S., Liang, Q., Zeng, X. & Li, T. 2018 Study of the effect of pyrolysis temperature on the Cd^{2+} adsorption characteristics of biochar. *Appl. Sci.* **8**, 1019.

Khattri, S. D. & Singh, M. K. 2009 Removal of malachite green from dye wastewater using neem sawdust by adsorption. *J. Hazard Mater.* **167**, 1089–1094.

Latour, R. A. 2015 The Langmuir isotherm: a commonly applied but misleading approach for the analysis of protein adsorption behavior. *J. Biomed. Mater. Res. A* **103**, 949–958.

Lyu, H., Gao, B., He, F., Zimmerman, A. R., Ding, C., Tang, J. & Crittenden, J. C. 2018 Experimental and modeling investigations of ball-milled biochar for the removal of aqueous methylene blue. *Chem. Eng. J.* **335**, 110–119.

Mosa, A., El-Ghamry, A. & Tolba, M. 2018 Functionalized biochar derived from heavy metal rich feedstock: phosphate recovery and reusing the exhausted biochar as an enriched soil amendment. *Chemosphere* **198**, 351–363.

Özer, D., Dursun, G. & Özer, A. 2007 Methylene blue adsorption from aqueous solution by dehydrated peanut hull. *J. Hazard. Mater.* **144**, 171–179.

Rafatullah, M., Sulaiman, O., Hashim, R. & Ahmad, A. 2010 Adsorption of methylene blue on low-cost adsorbents: a review. *J. Hazard. Mater.* **177**, 70.

Sadaf, S. & Bhatti, H. N. 2014 Batch and fixed bed column studies for the removal of Indosol Yellow BG dye by peanut husk. *J. Taiwan Inst. Chem. Eng.* **45**, 541–553.

Salleh, M. A. M., Mahmoud, D. K., Karim, W. A. W. A. & Idris, A. 2011 Cationic and anionic dye adsorption by agricultural solid wastes: a comprehensive review. *Desalination* **280**, 1–13.

Smith, Y. R., Bhattacharyya, D., Willhard, T. & Misra, M. 2016 Adsorption of aqueous rare earth elements using carbon black derived from recycled tires. *Chem. Eng. J.* **296**, 102–111.

Tan, I. A. W., Hameed, B. H. & Ahmad, A. L. 2007 Equilibrium and kinetic studies on basic dye adsorption by oil palm fibre activated carbon. *Chem. Eng. J.* **127**, 111–119.

Tan, I. A. W., Ahmad, A. L. & Hameed, B. H. 2008 Adsorption of basic dye on high-surface-area activated carbon prepared from coconut husk: equilibrium, kinetic and thermodynamic studies. *J. Hazard. Mater.* **154**, 337–346.

Vyavahare, G. D., Gurav, R. G., Jadhav, P. P., Patil, R. R., Aware, C. B. & Jadhav, J. P. 2018 Response surface methodology optimization for sorption of malachite green dye on sugarcane bagasse biochar and evaluating the residual dye for phyto and cytogenotoxicity. *Chemosphere* **194**, 306–315.

Yi, S., Gao, B., Sun, Y., Wu, J., Shi, X., Wu, B. & Hu, X. 2016 Removal of levofloxacin from aqueous solution using rice-husk and wood-chip biochars. *Chemosphere* **150**, 694–701.

First received 13 November 2018; accepted in revised form 23 April 2019. Available online 2 May 2019